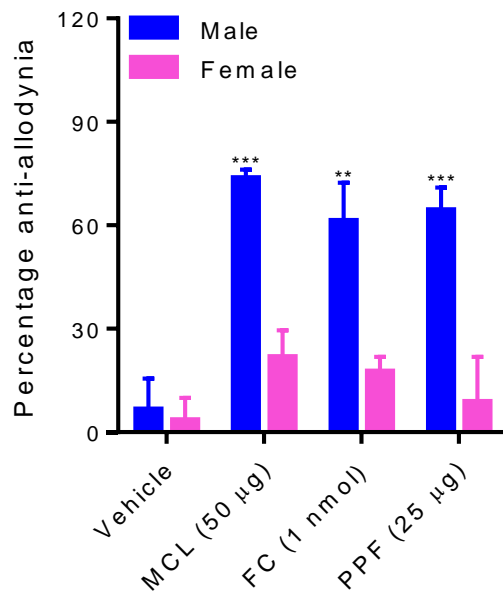


Supplementary Figure 1

Dose-dependent reversal of SNI-induced allodynia by intrathecal glial inhibitors in male but not female mice.

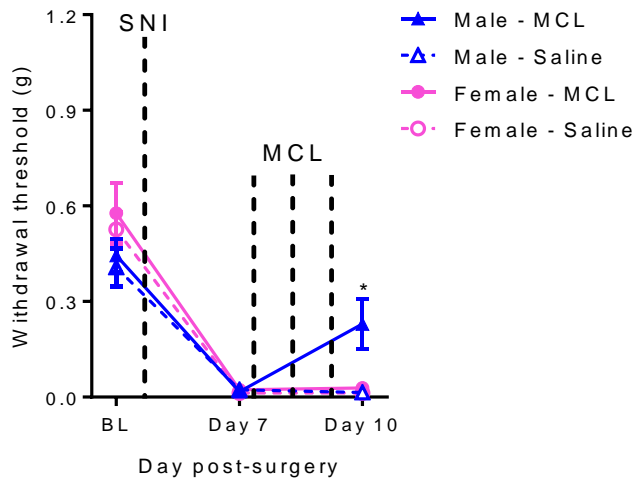
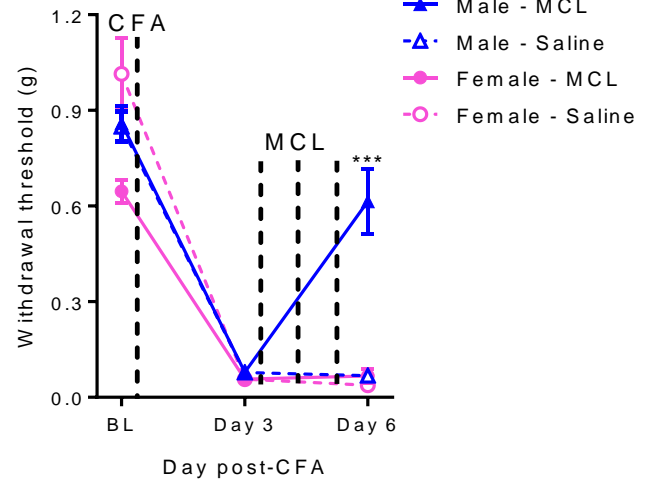
Reversal of SNI-induced allodynia by the glial inhibitors minocycline (MCL; **a**), fluorocitrate (FC; **b**) and propentofylline (PPF; **c**). Symbols represent mean \pm SEM percentage of maximum possible anti-allodynia (see Methods); $n=4-6$ mice/dose/sex/drug. ANOVAs revealed significant main effects of sex in each case (MCL: $F_{1,23} = 15.3$, $p=0.001$; FC: $F_{1,19} = 19.3$, $p<0.001$; PPF: $F_{1,26} = 66.7$, $p<0.001$). *** $p<0.001$ compared to female mice.



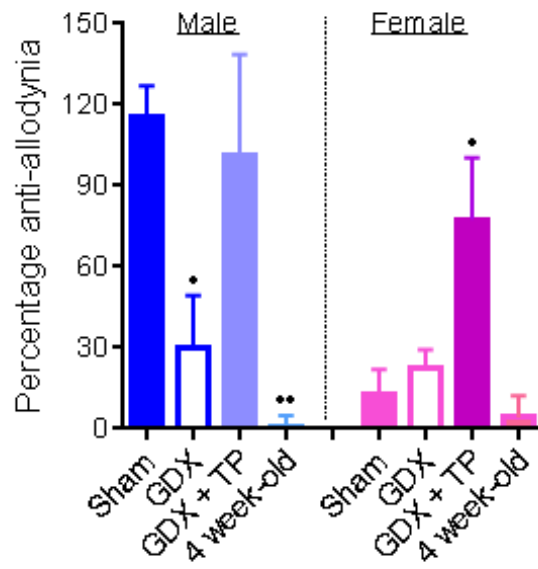
Supplementary Figure 2

Reversal of complete Freund's adjuvant (CFA)-induced mechanical allodynia by intrathecal glial inhibitors minocycline (MCL), fluorocitrate (FC) and propentofylline (PPF) in male but not female mice.

Bars represent mean \pm SEM percentage anti-allodynia; $n=5-7$ mice/sex/drug. All three glial inhibitors reversed allodynia in male but not female mice (MCL: $t_7 = 5.7$, $p < 0.001$; FC: $t_{11} = 3.4$, $p = 0.005$; PPF: $t_8 = 3.8$, $p = 0.005$). ** $p < 0.01$, *** $p < 0.001$ compared to female mice.

a. SNI**b. CFA****Supplementary Figure 3****Repeated systemic (i.p.) injections of minocycline (MCL) reverse SNI- and CFA-induced mechanical allodynia in male but not female mice.**

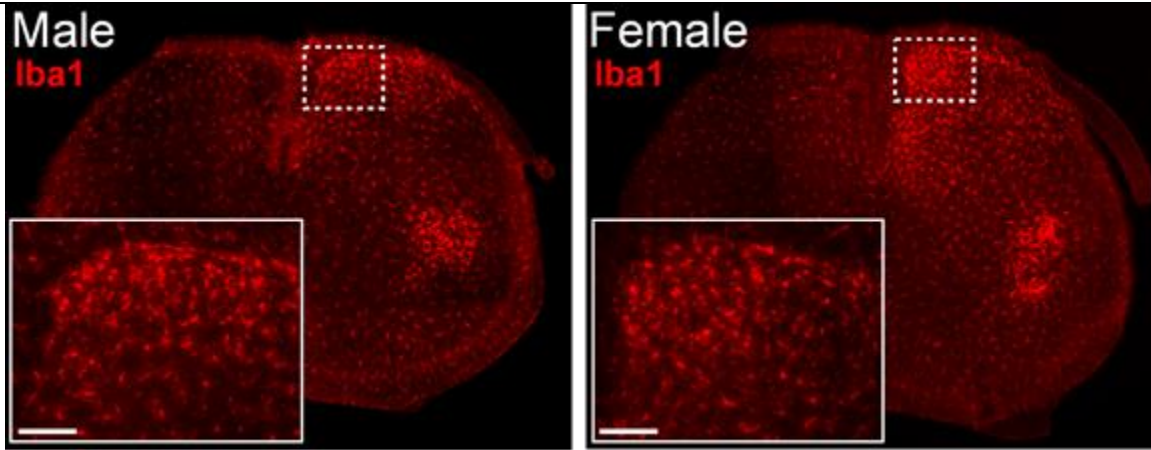
Symbols represent mean \pm SEM mechanical withdrawal thresholds (g) before (BL) and after SNI surgery (a) or CFA injection (b), and one day after three daily injections of MCL at 25 mg/kg/day (i.p.); $n=6-8$ mice/sex/drug in each experiment. In both experiments, a significant sex \times drug \times repeated measure (post-BL time points only) was observed ($F_{1,20} = 7.6$, $p=0.01$; $F_{1,26} = 68.0$, $p<0.001$, respectively). * $p<0.05$, *** $p<0.001$ compared to all other groups. Single injections of MCL produced no effects even at high doses (data not shown); repeated injections have previously shown to increase the anti-allodynic efficacy of MCL (Nazemi et al., Pharmacol. Biochem. Behav., 2012). Note that these observations are in contradiction to those of Bastos and colleagues, who observed partial reversal of chronic constriction injury (CCI)-mediated mechanical allodynia by 100 mg/kg minocycline in female C57BL/6 mice (Bastos et al., Neurosci. Lett., 543:157-162, 2013) and partial reversal of late-phase (15–30 min post-injection) formalin test responding by 50 and 100 mg/kg minocycline in male and female mice (Bastos et al., Neurosci. Lett., 553:110-114, 2013). In experiments by another group, 50 mg/kg minocycline was found to reverse thermal hyperalgesia induced by interleukin-1 β in female heterozygous G-protein-coupled receptor kinase 2 (GRK2) mutant mice on a C57BL/6 genetic background (Willemen et al., Pain, 2010). It is unclear whether the differences are due to assay, dose, measures or test parameters.



Supplementary Figure 4

Testosterone-dependence of the efficacy of minocycline in reversing CFA-induced allodynia.

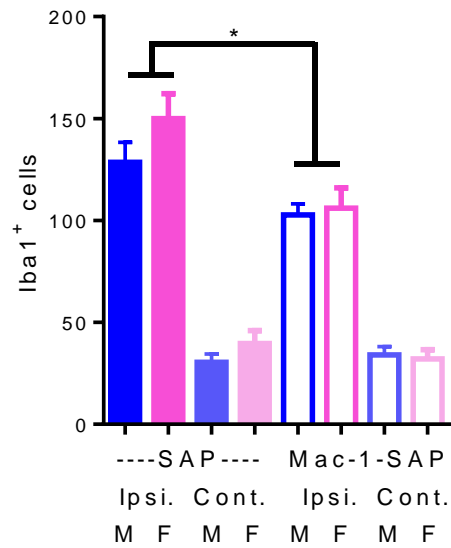
ANOVA revealed a significant sex x hormonal condition interaction ($F_{3,24} = 3.9, p=0.02$). Minocycline (50 μg) was ineffective in castrated male mice (male GDX) and young (4 week-old) mice of both sexes; its efficacy was reinstated in gonadectomized (GDX; castrated or ovariectomized) mice of both sexes given testosterone propionate replacement (GDX + TP). Bars represent mean \pm SEM percentage anti-allodynia ($n=4$ mice/sex/hormonal condition).



Supplementary Figure 5

Spinal microgliosis 7 days after SNI in male (left) and female (right) mice.

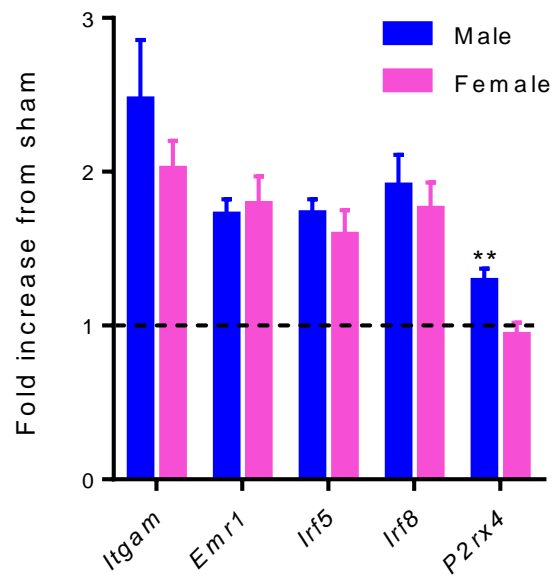
Microglial proliferation is shown by Iba1 immunoreactivity (red). Insets are high power images of transverse sections of lumbar spinal cord. Dotted region shows region of high power image. Scale bar = 100 μ m. No sex differences were seen in NeuN-positive or GFAP-positive cells (data not shown; also see **Supplementary Fig. 8c**).



Supplementary Figure 6

Microglial depletion by intrathecal Mac-1-saporin treatment in male and female mice.

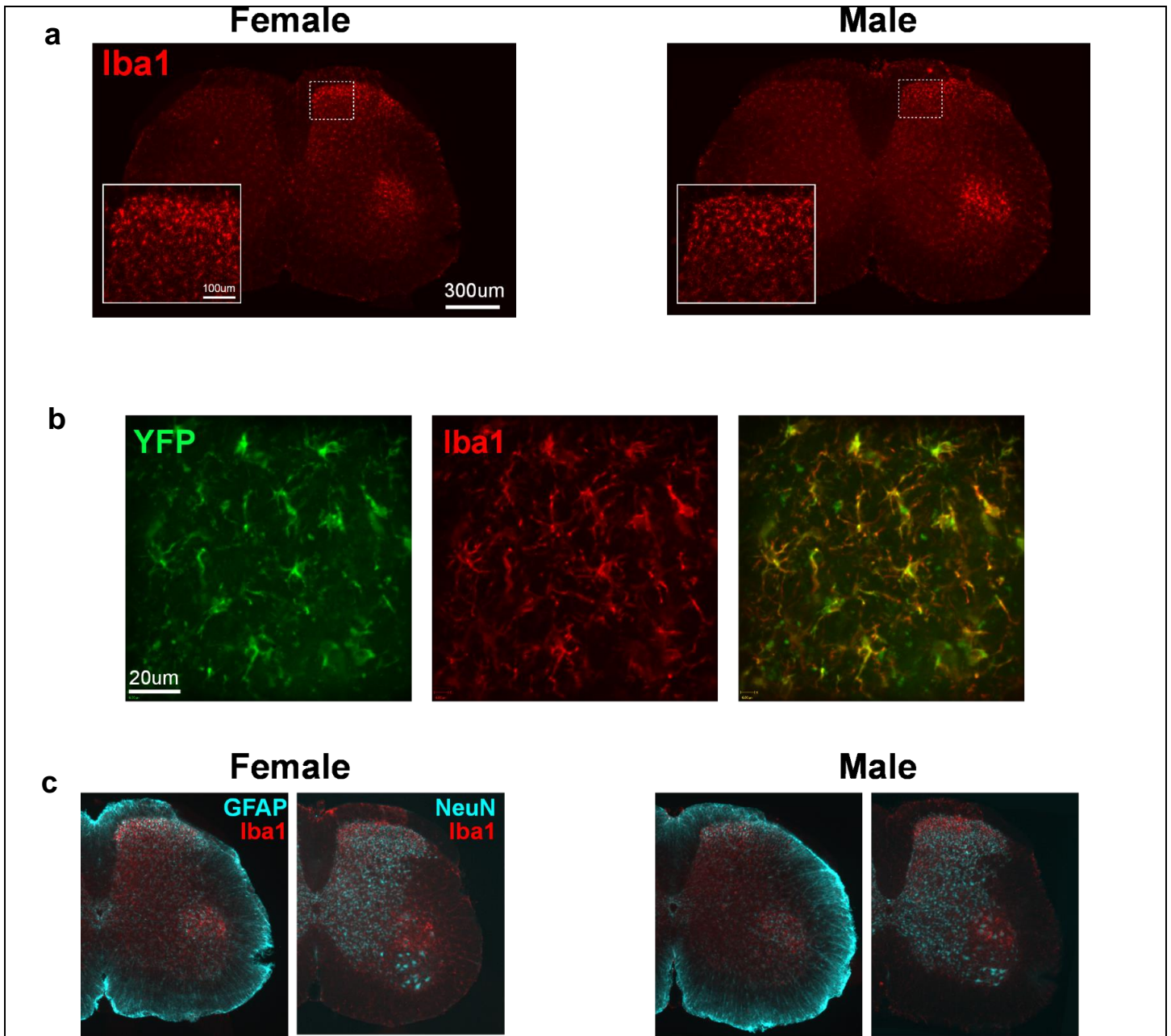
Depletion of microglia ipsilateral (Ipsi.) to the SNI (7 days post-surgery) in both male (M) and female (F) mice 4 h after treatment with Mac-1-saporin (Mac-1-SAP) toxin compared to mice treated with saporin (SAP) vehicle. Bars represent mean \pm SEM Iba1-positive (Iba1⁺) cells in the lumbar spinal cord dorsal horn ($n=5$ mice/sex/condition). Cont.=contralateral. Similar microglial depletion ($\approx 25\%$) was observed in both sexes (male: $t_8 = 2.4$, $p=0.02$; female: $t_8 = 2.8$, $p=0.001$). * $p<0.05$.



Supplementary Figure 7

SNI upregulates expression of the *Itgam* (CD11b), *Emr1* (F4/80; a surface marker for microglia), *Irf5*, and *Irf8* genes (see below) in the dorsal horn of the spinal cord equally in both sexes, but only upregulates the *P2rx4* gene (P2X₄R) in male mice.

Symbols represent normalized $2^{-\Delta\Delta Ct}$ values ($n=8$ biological replicates/sex/surgical condition) compared to the average of four reference genes. All male vs. female t -test values $p>0.40$, except for *P2rx4*: $t_{14} = 3.5$, $p=0.003$. ** $p<0.01$ compared to other sex. In male mice, P2X₄R gene expression is under the transcriptional control of interferon regulatory factors 5 and 8 (IRF5 and IRF8). Following peripheral nerve injury, IRF8 is upregulated and directs gene expression changes associated with microglial reactivity, including motility, chemotaxis, Iba1 expression and increases in IRF5 (Masuda et al., Nat. Commun. 2014; Masuda et al., Purinergic Signal., 2014). IRF5 binds directly to the promoter region of *P2rx4* and has direct transcriptional control over it, resulting in *de novo* expression of microglial P2X₄R after peripheral nerve injury. Following nerve injury, *Irf8* is upregulated (and, as shown above, equally in males and females), with a consequent spinal microglial proliferation and upregulation of *Itgam* (and *Aif1*, which codes for Iba1). *Irf5* is in turn upregulated and, in males but not females, leads to increased *P2rx4* gene expression. However, in females, despite the increased IRF5, *P2rx4* expression is unaffected. This pattern of gene expression changes after nerve injury shows the point of divergence in the cellular and molecular pathways underlying neuropathic pain in male and female mice lies at the induction of P2X₄R.

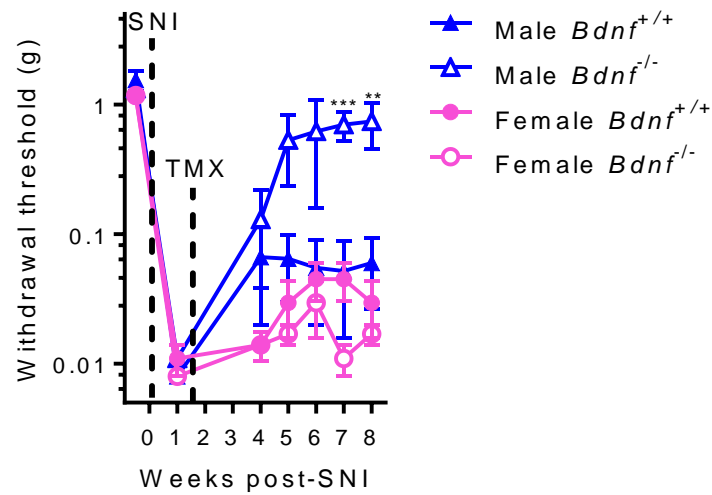


Supplementary Figure 8

Nerve injury-induced microglia responses are present in microglial-specific *Bdnf* mutant mice of both sexes.

a) Spinal cord dorsal horn microgliosis following SNI in *Cx3cr1^{CreER} x loxP-Bdnf* mice. Insets are high power images taken from the ipsilateral dorsal horn of the spinal cords from female (left) and male (right) mice. Microglia were labelled with Iba1 (red). Both males and females show the characteristic microglial proliferation around the central terminals of peripherally axotomised sciatic afferents. **b)** Microglial-specific *Bdnf* mutant express a YFP IRES element. YFP (green) colocalizes directly with microglia (Iba1; red) in the spinal cord. **c)** Other cellular populations are identical in male and female microglial-specific *Bdnf* mutant mice after SNI. Astrocytes and neuronal nuclei are shown by GFAP and NeuN immunohistochemistry (both blue), respectively.

Cx3cr1^{CreER}-*Bdnf* Mutant (Reversal)

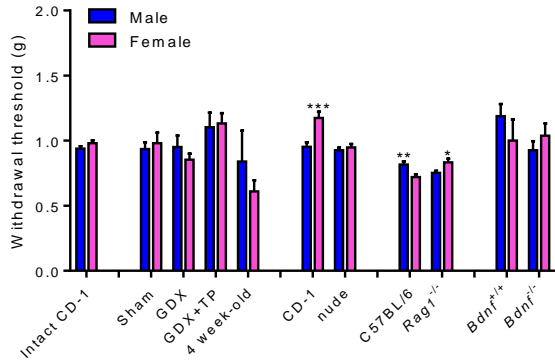


Supplementary Figure 9

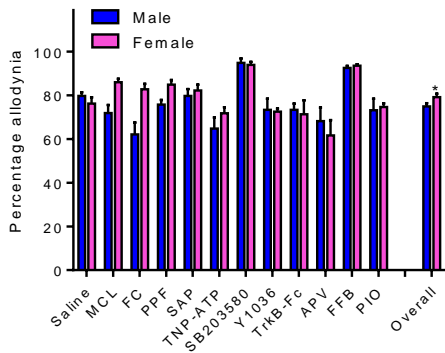
Reversal of developed SNI-induced mechanical allodynia in male *Bdnf*^{-/-} mice.

Reversal of SNI in male mutant mice (*Bdnf*^{-/-}) in which central nervous system microglial BDNF is deleted following tamoxifen (TMX) treatment, but not male *Bdnf*^{+/+} or female mice of both genotypes. Repeated measures ANOVA revealed a significant sex x genotype x repeated measures interaction: $F_{5,65} = 3.1$, $p=0.01$. Symbols represent mean \pm SEM absolute withdrawal thresholds from von Frey filaments before surgery, 1 week post-surgery, and 4–8 weeks post-TMX treatment ($n=4$ mice/sex/genotype). ** $p<0.01$, *** $p<0.001$ compared to all other groups.

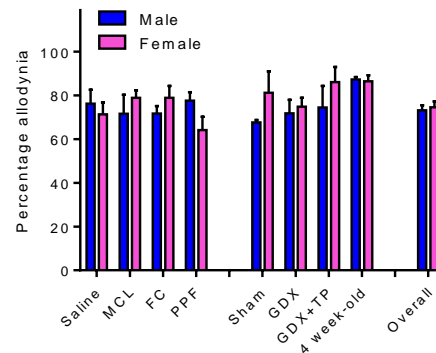
a. Baseline latencies



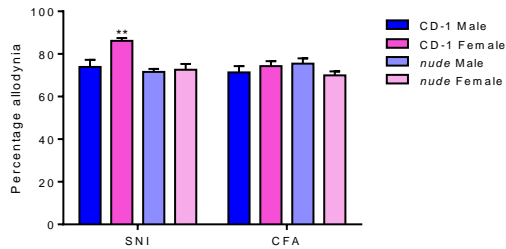
b. SNI - percentage allodynia at Day 7



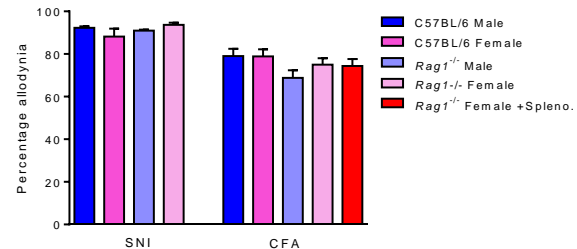
c. CFA - percentage allodynia at Day 3



d. nude



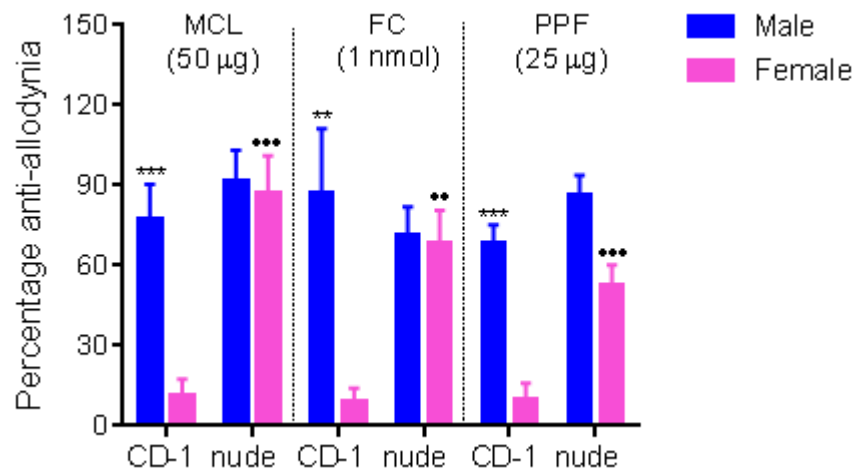
e. Rag1



Supplementary Figure 10

Quantitative sex differences in baseline mechanical sensitivity (a) and SNI- and CFA-induced mechanical allodynia (b-e) in various experiments.

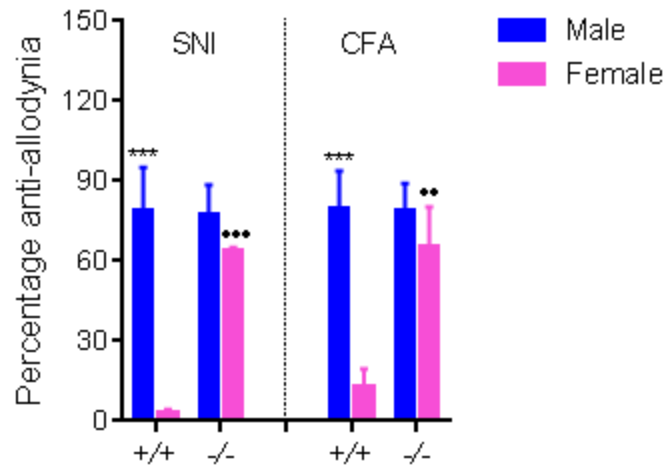
Bars in **a** represent mean \pm SEM baseline von Frey thresholds of various mouse populations by sex. Bars in **b,c** represent mean \pm SEM mechanical allodynia in CD-1 mice measured at 7 days post-SNI surgery (**b**) or 3 days post-CFA injection (**c**) in various drug conditions or mouse populations by sex. Bars in **d,e** represent mean \pm SEM mechanical allodynia measured at 7 days post-SNI surgery or 3 days post-CFA injection in CD-1 (wildtype) and *nude* mice (**d**) and C57BL/6 (wildtype) and *Rag1*^{-/-} mice (**e**). * p <0.05, ** p <0.01, *** p <0.001 compared to other sex within-genotype or condition by (uncorrected) *t*-test. The slightly but significantly increased neuropathic allodynia of female CD-1 mice (see graphs **b,d**) has not been observed previously, but is well-documented (Coyle et al., Neurosci. Lett. 1995; Dominguez et al., Eur. J. Pain, 2012; Dina et al., Neuroscience, 2007; LaCroix-Fralish et al., Neuroscience 2006; LaCroix-Fralish et al., Pain, 2005; Tail et al., Pharmacol. Biochem. Behav., 2001), although strain-dependent (DeLeo & Rutkowski, Neurosci. Lett., 2000), in the rat.



Supplementary Figure 11

Female *nude* mice “switch” to a microglial-dependent system in the mediation of CFA allodynia.

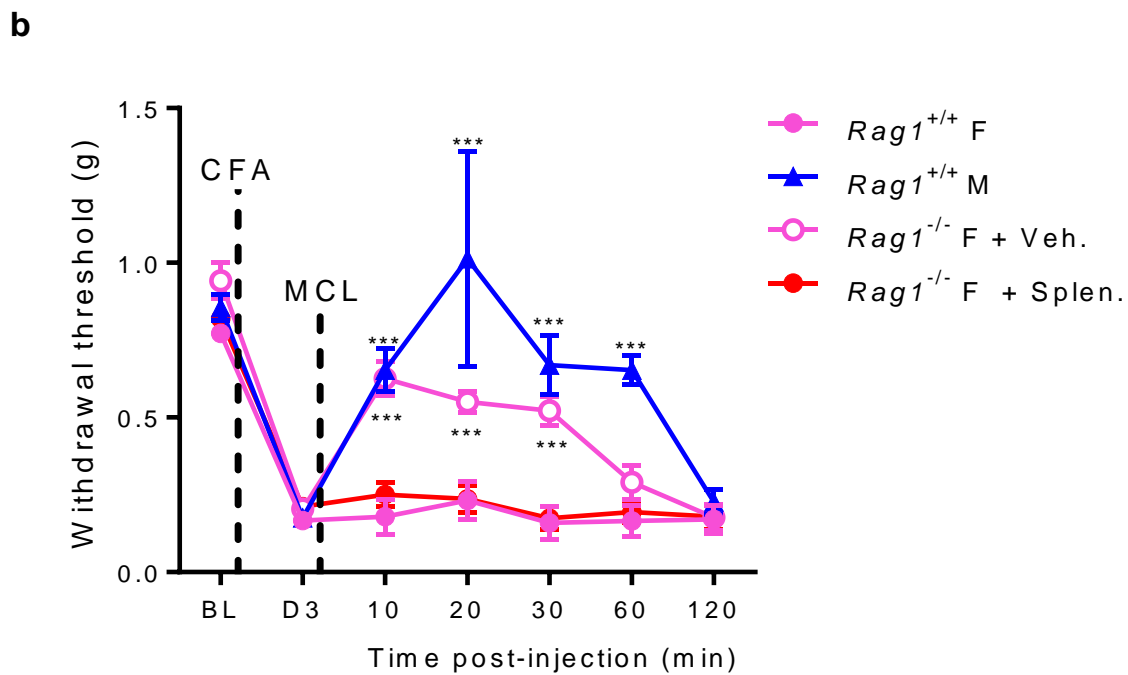
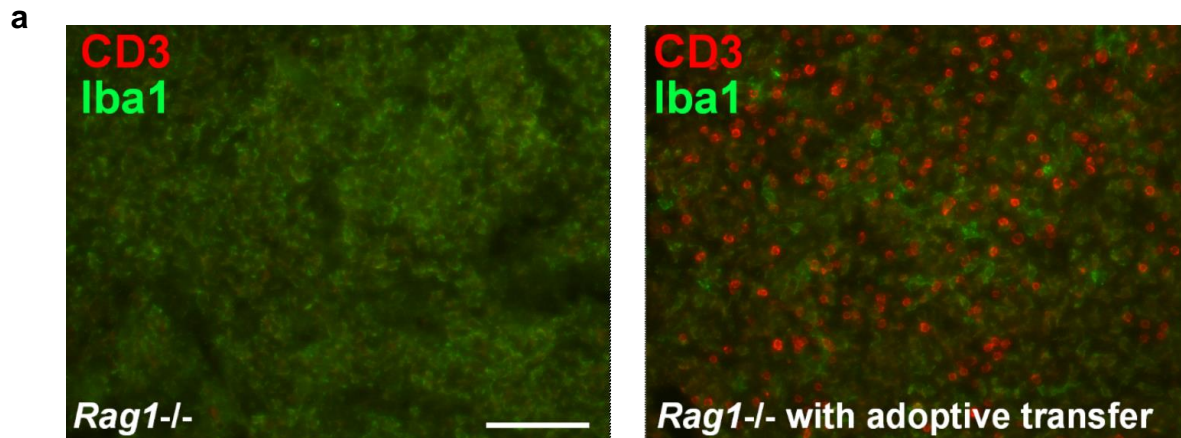
Graph shows reversal of mechanical allodynia 3 days after CFA by i.t. administered glial inhibitors minocycline (MCL), fluorocitrate (FC) and propentofylline (PPF) in male but not female CD-1 mice, but in immunocompromised *nude* mice of both sexes. Bars represent mean \pm SEM percentage of maximum reversal of allodynia (% anti-allodynia) ($n=4-7$ mice/sex/drug/genotype). ANOVAs showed significant genotype x sex interactions in all cases (MCL: $F_{1,19} = 7.1$, $p=0.01$; FC: $F_{1,16} = 7.7$, $p=0.01$; PPF: $F_{1,22} = 4.2$, $p=0.05$). ** $p < 0.01$, *** $p < 0.001$ compared to same-strain female mice by *t*-test. ** $p < 0.01$, *** $p < 0.001$ compared to same-sex CD-1 mice by *t*-test.



Supplementary Figure 12

Female *Rag1*^{-/-} mice “switch” to a microglial-dependent system in the mediation of SNI and CFA allodynia.

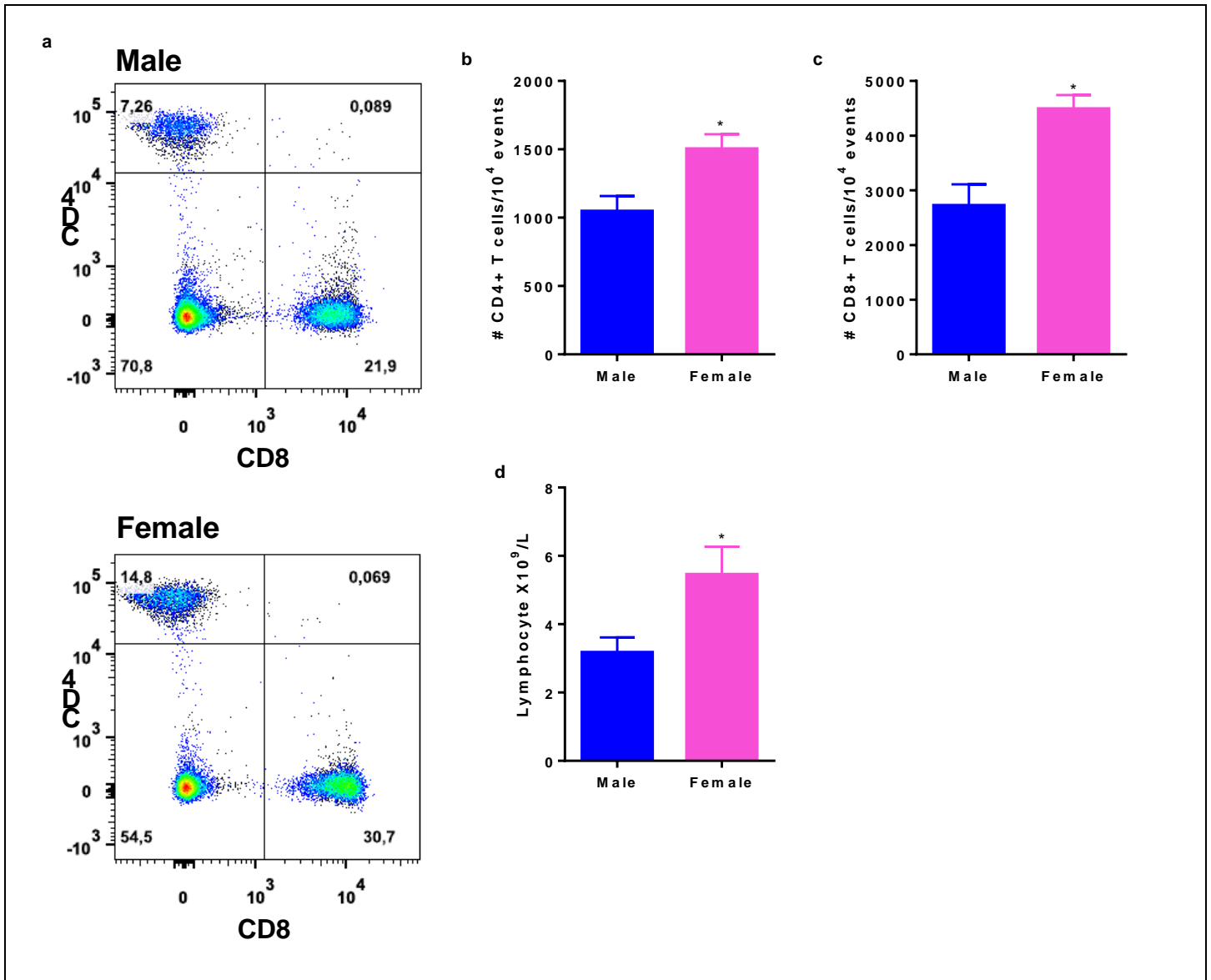
Graph shows reversal of mechanical allodynia after SNI or CFA by i.t. minocycline (MCL; 50 μ g) in male but not female wildtype (+/+; C57BL/6) mice, but in immunocompromised *Rag1*^{-/-} (-/-) mice of both sexes. Bars represent mean \pm SEM percentage of maximum reversal of allodynia (% anti-allodynia) ($n=6-8$ mice/sex/genotype). ANOVAs revealed significant genotype x sex interactions in both cases (SNI: $F_{1,20} = 9.5$, $p=0.006$; CFA: $F_{1,24} = 4.7$, $p=0.04$). *** $p<0.001$ compared to same-genotype female mice by t -test. ** $p<0.01$, *** $p<0.001$ compared to same-sex +/+ mice by t -test.



Supplementary Figure 13

Adoptive transfer of splenocytes into female *Rag1*^{-/-} mice reinstates their use of the female glial-independent pathway.

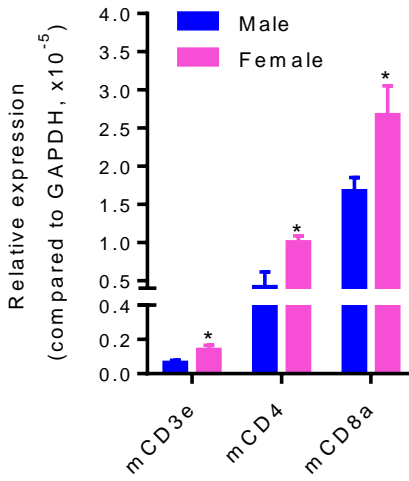
a) Successful repopulation by adoptive transfer. Spleen sections taken from a female *Rag1*^{-/-} mouse (left) and a female *Rag1*^{-/-} mouse following adoptive splenocyte transfer (right). Spleen macrophages are labelled in green (Iba1) and repopulated T-cells in red (CD3). Scale bar = 200 μ m. **b)** Adoptive transfer of splenocytes (Splen.) from immunocompetent female (F) *Rag1*^{+/+} into immunocompromised female *Rag1*^{-/-} mice (i.e., *Rag1*^{-/-} F + Splen. condition) restores the male (M)-like ability of i.t. MCL (50 μ g; 3 days after injection; D3) to reverse CFA allodynia. *Rag1*^{-/-} F + Veh. indicates mutant females which received the adoptive transfer vehicle without splenocytes. Symbols represent mean \pm SEM 50% withdrawal threshold from von Frey filaments before CFA (BL), 3 days after CFA, pre-MCL injection (D3), and 10–120 min post-injection of MCL ($n=4-6$ mice/sex/condition except for adoptive transfer group, $n=10$). Repeated measures ANOVA revealed a significant group \times repeated measures interaction: $F_{15,100} = 5.8$, $p < 0.001$. *** $p < 0.001$ compared to *Rag1*^{+/+} F and *Rag1*^{-/-} F + Splen. groups by Tukey's posthoc test.



Supplementary Figure 14

Female mice have a larger pool of T-cells in the blood than do male mice.

The number of CD4⁺ and CD8⁺ T cells in the blood of male and female naïve mice was quantified using FACS analysis. **a)** Representative examples of flow cytometric analysis of peripheral CD4⁺ and CD8⁺ T-cells in the blood of male (top) and female (bottom) mice. **(b,c)** histograms represent the FACS analysis (bars represent mean ± SEM counts) of CD4⁺ **(b)** and CD8⁺ **(c)** T-cells in the blood obtained from 3 naïve mice per sex. Female mice have more CD4⁺ ($t_4 = 2.9$, $p=0.04$) and CD8⁺ ($t_4 = 3.8$, $p=0.02$) T-cells than males. **d)** The number of lymphocytes in the blood of male and female mice was further confirmed using standard complete blood counting (CBC) ($n=6$ mice/sex; bars represent mean ± SEM counts); female mice exhibited higher numbers of lymphocytes ($t_{10} = 2.5$, $p=0.03$). * $p<0.05$ compared to males.



Supplementary Figure 15

Higher expression of T-cell markers in the lumbar spinal cord dorsal horns of female versus male CD-1 mice 7 days after SNI.

Bars represent Ct values \pm SEM ($n=5-6$ mice/sex), expressed relative to the housekeeping gene, *Gapdh*. CD3e: $t_8 = 2.8, p=0.02$; CD4: $t_6 = 3.3, p=0.02$; CD8a: $t_9 = 2.2, p=0.05$. * $p<0.05$ compared to males.